Soluble IL7Rα potentiates IL-7 bioactivity and promotes autoimmunity

Wangko Lundström[a,b], Steven Highfill[a], Scott T. R. Walsh[c], Stephanie Beq[d], Elizabeth Morse[a], Ingrid Kockum[b], Lars Alfredsson[e], Tomas Olsson[b], Jan Hillert[b], and Crystal L. Mackall[a,1]

[a]Pediatric Oncology Branch, Center for Cancer Research, National Cancer Institute, Bethesda, MD 20892; [b]Department of Clinical Neuroscience, Karolinska Institutet, Stockholm, Sweden; [c]Department of Cell Biology and Molecular Genetics, University of Maryland, College Park and Institute for Bioscience and Biotechnology Research, Department of Cell Biology and Molecular Genetics, University of Maryland, Rockville, MD 20850; [d]Cytheris SA, 92130 Issy le Moulineaux, France; and [e]Institute of Environmental Medicine, Karolinska Institutet, 17176 Stockholm, Sweden

Edited by Tak W. Mak, The Campbell Family Institute for Breast Cancer Research, Ontario Cancer Institute at Princess Margaret Hospital, University Health Network, Toronto, ON, Canada, and approved April 1, 2013 (received for review January 3, 2013)

Human soluble interleukin-7 receptor (sIL7R)α circulates in high molar excess compared with IL-7, but its biology remains unclear. We demonstrate that sIL7Rα has moderate affinity for IL-7 but does not bind thymic stromal lymphopoietin. Functionally, sIL7Rα competes with cell-associated IL-7 receptor to diminish excessive IL-7 consumption and, thus, enhances the bioactivity of IL-7 when the cytokine is limited, as it is presumed to be in vivo. IL-7 signaling in the presence of sIL7Rα also diminishes expression of CD95 and suppressor of cytokine signaling 1, both regulatory molecules. Murine models confirm diminished consumption of IL-7 in the presence of sIL7Rα and also demonstrate a potentiating effect of sIL7Rα on IL-7–mediated homeostatic expansion and experimental autoimmune encephalomyelitis exacerbation. In multiple sclerosis and several other autoimmune diseases, *IL7R* genotype influences susceptibility. We measured increased sIL7Rα levels, as well as increased IL-7 levels, in multiple sclerosis patients with the predisposing *IL7R* genotype, consistent with diminished IL-7 consumption in vivo. This work demonstrates that sIL7Rα potentiates IL-7 bioactivity and provides a basis to explain the increased risk of autoimmunity observed in individuals with genotype-induced elevations of sIL7Rα.

immunology | soluble receptors | tolerance

IL-7 plays a fundamental role in T-cell development, peripheral T-cell homeostasis, and immune tolerance. Unlike activation cytokines, where cytokine production and receptor expression mediate transient effects following immune activation, tonic IL-7 signals are continuously delivered to nearly all T cells, and IL-7 provides continuous survival signals to naïve T cells (1, 2). Under normal conditions, IL-7 is a limited resource (3), but diminished IL-7 consumption in lymphopenic hosts leads to elevated IL-7 levels that enhance proliferative responses to weak self-antigens (4, 5), thus driving homeostatic proliferation (6). Proliferative responses to self-antigens can also be induced by pharmacologic dosing of IL-7 in lymphoreplete hosts (7, 8), and increases in IL-7 availability, induced by lymphopenia (9), pharmacologic administration (10), or constitutive overexpression in IL-7 transgenic mice (11) predispose to autoimmune disease. IL-7 has been implicated as a cofactor in several autoimmune diseases, including experimental autoimmune encephalitis (12, 13), autoimmune colitis (14), autoimmune diabetes (15), and lupus (16). Thus, IL-7 signaling contributes to autoimmunity in several models, and enhanced IL-7 signaling alone is sometimes sufficient to break immune tolerance.

The cell-associated IL-7 receptor complex consists of IL-7 receptor alpha (IL7Rα; CD127) and the common γ chain (γc; CD132). IL7Rα also associates with thymic stromal lymphopoietin (TSLP) receptor (TSLPR) (CRLF2) to form the TSLP receptor complex. Many soluble receptors are conserved across species, and several studies have demonstrated fundamental roles for soluble cytokine receptors in modulating cytokine activity (17). Biological functions of soluble receptors range from antagonistic [e.g., soluble IL-1RII (18)] to half-life prolonging [e.g., soluble IL-6Rα (19)] and potentiating [e.g., soluble IL-15Rα (20)]. Soluble IL7Rα (sIL7Rα) was identified in 1990 coincident with cloning of human cell-associated IL7Rα, and sIL7Rα is known to circulate in nanomolar concentrations (21–24), but, to date, the biological function of sIL7Rα remains unclear. There are two primary mechanisms through which soluble cytokine receptors can be produced (17): shedding of membrane-bound receptors [e.g., TNF receptor 2 (25)] and alternative splicing leading to a protein lacking the transmembrane domain [e.g., IL-9Rα (26)]. Previous biochemical studies have demonstrated that sIL7Rα present in human plasma is primarily derived from alternative splicing and comprises an isoform lacking exon 6 (Δ6IL7Rα), as well as a unique 26-aa sequence as a result of a frame shift and a premature stop codon (24) (Fig. S1). One previous manuscript concluded that sIL7Rα served to inhibit IL-7 signaling (22), but this focused solely on very early time points in vitro and lacked in vivo studies. Furthermore, the previous study used an IL7Rα-Fc fusion protein, wherein the binding domain is comprised exclusively of the extracellular domain (ECD), rather than the protein derived from alternative splicing, which is the predominant circulating form found in humans. Thus, despite the importance of soluble receptors in several model systems, the biology of sIL7Rα has remained poorly understood.

The C allele of a single-nucleotide polymorphism (SNP) in exon 6 of *IL7R* (rs6897932), hereafter referred to as *IL7R**C, is associated with increased susceptibility to multiple sclerosis (MS) (27–30). Furthermore, high linkage disequilibrium demonstrates that *IL7R**C is nearly always coinherited with increased risk alleles identified in primary biliary cirrhosis (rs860413 A allele), ulcerative

Significance

Many genes have been shown to influence the risk of developing multiple sclerosis (MS); however, the biological processes responsible are not clear. We found that a genetic polymorphism associated with increased MS risk is responsible for potentiating the effects of a cytokine named interleukin (IL)-7 by securing its availability and bioactivity over time. This effect was mediated by an isoform of the IL-7 receptor that circulates at high levels in blood. IL-7 is an important factor for T-cell maturation and proliferation, and, hence, its association to MS, which is an autoimmune disease, is not surprising.

Author contributions: W.L., S.H., S.T.R.W., J.H., and C.L.M. designed research; W.L., S.H., S.T.R.W., S.B., and E.M. performed research; S.T.R.W., S.B., I.K., L.A., T.O., and J.H. contributed new reagents/analytic tools; W.L., S.H., S.T.R.W., S.B., E.M., and C.L.M. analyzed data; and W.L. and C.L.M. wrote the paper.

The authors declare no conflict of interest.

This article is a PNAS Direct Submission.

[1]To whom correspondence should be addressed. E-mail: mackallc@mail.nih.gov.

This article contains supporting information online at www.pnas.org/lookup/suppl/doi:10.1073/pnas.1222303110/-/DCSupplemental.

colitis (rs3194051 G allele), and sarcoidosis (rs10213865 A allele) (31). Previous studies demonstrated that the autoimmunity predisposing *IL7R* genotype increases the rate of IL7Rα mRNA splicing (27, 32) and results in increased levels of sIL7Rα (23), thus potentially associating increased sIL7Rα levels with an increased susceptibility to autoimmunity (31). However, in light of the voluminous data implicating IL-7 as a cytokine capable of breaking self-tolerance and as a cofactor in a variety of autoimmune diseases, it was difficult to reconcile this observation with the only previous published report on the biologic effects of sIL7Rα, which concluded that sIL7Rα antagonizes IL-7 bioactivity. We, therefore, sought to carefully elucidate the biologic effects of sIL7Rα and to determine how genotype mediated differential rates of IL7Rα mRNA splicing could impact IL-7 bioactivity and susceptibility to autoimmune disease.

Results

sIL7Rα Binds IL-7 but Not TSLP. To study the biology of sIL7Rα, we produced the protein encoded by the Δ6IL7Rα mRNA, as well as a protein comprised solely of the ECD of IL7Rα (IL7Rα-EC), which does not contain the unique 26-aa tail found in sIL7Rα and would be predicted to be identical to shed sIL7Rα. Using surface plasmon resonance, we measured binding affinities of both proteins for IL-7 and TSLP, ligands for cell-associated receptors containing IL7Rα (Fig. 1). The protein encoded by Δ6IL7Rα mRNA displays moderate affinity for rhIL-7 (K_d, 6.3 nM), which was 16-fold stronger than the binding affinity of IL7Rα-EC to rhIL-7 (K_d, 98 nM), primarily because of a faster k_1 rate constant (2.6×10^6 vs. 6.2×10^5 M/s; Fig. 1*A* vs. *C*). At concentrations up to 0.5 μM, we saw no binding between Δ6IL7Rα and TSLP (Fig. 1*B*), whereas moderate affinity (K_d, 53 nM) was measured between TSLP to TSLPR-EC (Fig. 1*D*). Based upon these studies, we conclude that immunobiologic effects of Δ6IL7Rα occur as a result of binding to IL-7 rather than TSLP. We further conclude that binding affinity of sIL7Rα to IL-7 is ∼1 log weaker than the picomolar binding affinity previously measured between IL-7 and the cell-associated IL7R complex (33–35).

sIL7Rα Enhances IL-7–Induced Survival of 2E8 Cells by Diminishing Consumption. To assess the effects of sIL7Rα on IL-7 bioactivity, we measured IL-7–mediated survival of 2E8, an IL-7–dependent murine pro–B-cell line, in the presence of rhIL7 (2,000 pg/mL) and varying concentrations of sIL7Rα. No effects were observed at early time points, but we observed a trimodal effect on day 12 of culture (Fig. 2*A*). The fact that effects were not apparent until a late time point led us to postulate that IL-7 consumption could be significantly impacted by the presence of sIL7Rα and that such an effect would become increasingly apparent with longer culture periods. At low molar ratios (≤128), cell survival was substantially diminished from baseline and from earlier time points, and we postulated that this reflected low IL-7 levels attributable to increasing IL-7 consumption over time. At middle molar ratios (256 and 512), we observed enhanced cell survival, and we postulated that this resulted from diminished IL-7 consumption leading to increased IL-7 availability and, thus, increased cell survival. Finally, at high molar ratios (≥1,024), we postulated that the large excess of sIL7Rα diminished free IL-7, thus preventing binding of IL-7 to its cell-associated receptor and leading to cell death.

To directly test the hypothesis that sIL7Rα modulates IL-7 consumption, we used the same model system but lowered the IL-7 concentration to 250–500 pg/mL and then assessed sIL7Rα-mediated effects on 2E8 survival and on IL-7 levels with a focus on molar ratios that mediated potentiation. Under these conditions, sIL7Rα plus IL-7 significantly increased 2E8 survival beginning on day 5 (Fig. 2*B*), and significantly increased IL-7

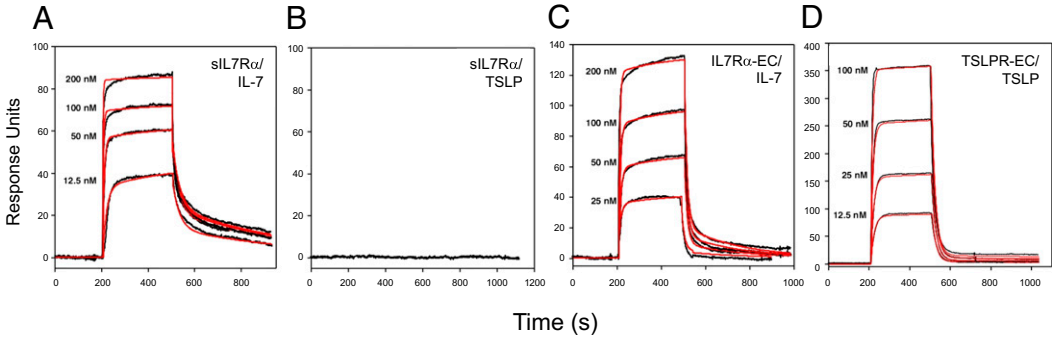

E

Binding constants for cytokine/receptor interactions					
	k_1 ($M^{-1}s^{-1}$)	k_{-1} (s^{-1})	k_2 (s^{-1})	k_{-2} (s^{-1})	k_d (nM)
IL-7/sIL7Rα	2.6×10^6	$3.3. \times 10^{-2}$	2.0×10^{-3}	2.0×10^{-3}	6.3
IL-7/IL7Rα-EC	6.2×10^5	7.7×10^{-2}	1.2×10^{-3}	4.4×10^{-3}	98
TSLP/sIL7Rα	[1]nd	[1]nd	[1]nd	[1]nd	[2]NB
TSLP/TSLPR-EC	6.1×10^5	4.1×10^{-2}	1.2×10^{-4}	4.6×10^{-4}	53

[1]not determined
[2] no measurable binding at 0.5uM TSLP

Fig. 1. sIL7Rα binds IL-7 but not TSLP. The binding kinetics for all of the cytokine/receptor interactions fit best to a two-step binding reaction model using two on-rate (k_1 and k_2) and off-rate (k_{-1} and k_{-2}) constants. (*A–D*) Surface plasmon resonance sensorgrams are shown for each designated protein pair. Black lines represent raw data and red lines represent the global fitting analysis of the sensorgrams to a two-step binding reaction model using ClampXP. (*E*) Summary of binding affinities measured in *A–D*. Experiments were performed in triplicate with errors on the order of 5–10% for the rate constants.

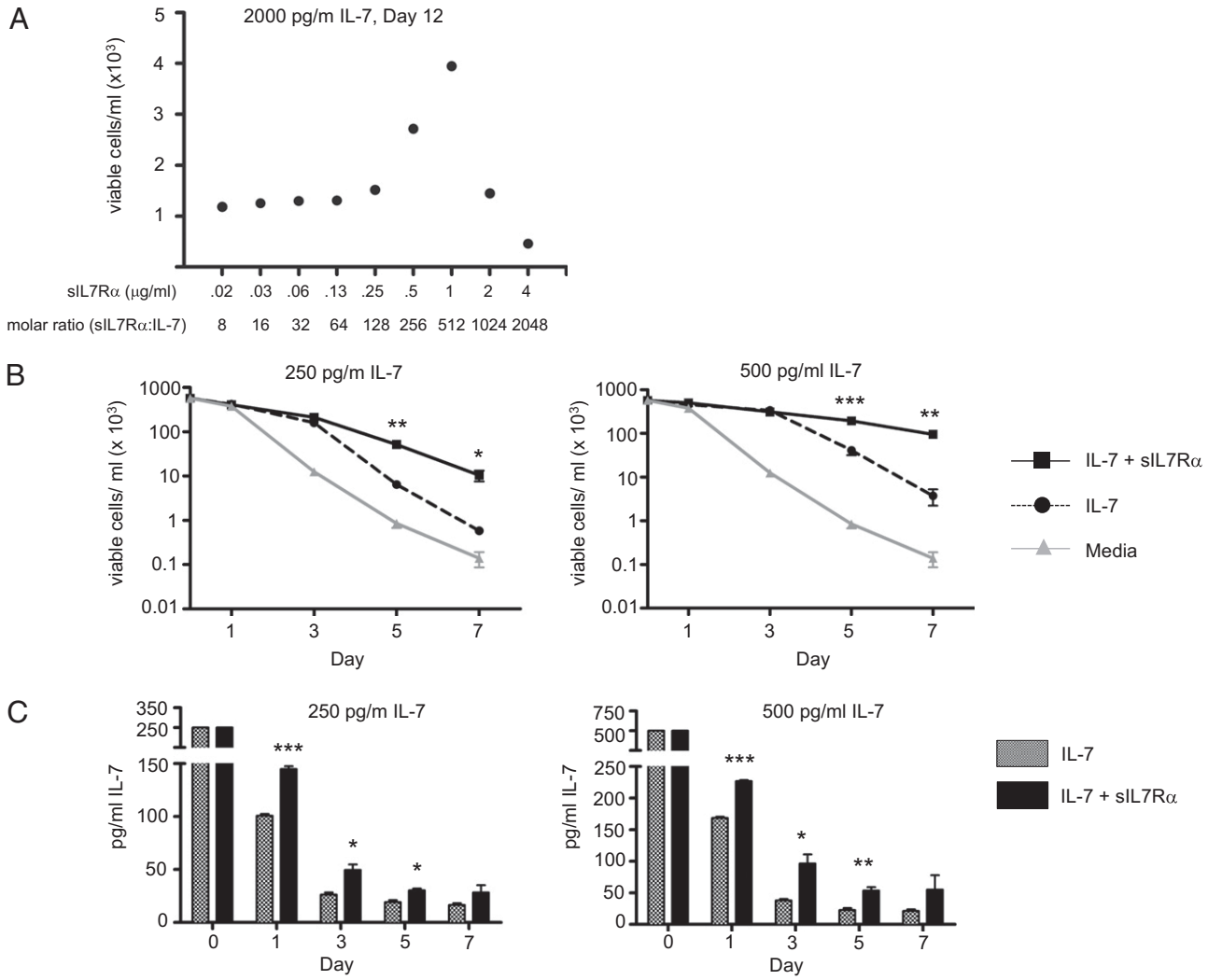

Fig. 2. sIL7RA potentiates IL-7–mediated survival and diminishes consumption of IL-7. (*A*) Survival of the IL-7–dependent cell line 2E8 was measured in the presence of rhIL-7 (2,000 pg/mL) plus varying concentrations of sIL7Rα. No effects were seen at any time point using molar ratios of 128:1 and below. However, on day 12, increased survival was observed at sIL7Rα:IL-7 molar ratios of 256–512:1, which was diminished at higher molar ratios. (*B*) Using lower concentrations of rhIL-7 [250 pg/mL (*Left*) and 500 pg/mL (*Right*)], survival of 2E8 from days 0–7 is shown with no cytokine, rhIL-7 alone, or sIL7Rα:rhIL7 molar ratio of 500:1. sIL7RA significantly increased survival on days 5 and 7 (*$P < 0.05$; **$P < 0.01$; ***$P < 0.001$). Error bars represent SEM of triplicate experiments. (*C*) IL-7 levels measured in the cultures described in *B*. Significantly increased IL-7 levels were measured in the presence of sIL7Rα on days 1, 3, and 5 of culture (*$P < 0.05$; **$P < 0.01$; ***$P < 0.001$). Error bars represent SEM of triplicate experiments. This experiment was performed three times with similar results.

levels were present in cultures containing sIL7Rα on days 1 through 5 (Fig. 2*C*). We observed no effect of sIL7Rα on IL-7 levels maintained at 37 °C in a serum-containing, but cell-free, system, ruling out the possibility that sIL7Rα diminished spontaneous or proteolytic degradation of IL-7. Furthermore, at the molar ratios used in this system, sIL7Rα had no effect on the accuracy of the IL-7 ELISA in measuring IL-7 levels. Therefore, sIL7Rα diminishes IL-7 consumption by IL7R expressing target cells, leading to enhanced IL-7 bioactivity in settings where IL-7 is limited.

sIL7Rα Modulates IL-7 Signaling in Human T Cells. The cell line 2E8 is an IL-7–dependent murine cell line, raising the possibility that these results could reflect a competitive disadvantage of cell-associated mouse IL7R complex for rhIL-7 binding. We, therefore, explored the effects of sIL7Rα on IL-7 signaling using human T cells. Using STAT5 phosphorylation as a readout of early IL7R signaling, 50:1 molar ratio of sIL7Rα:rhIL-7 had no effect, incomplete blockade was noted with 500:1 ratios, and at 5,000:1, sIL7Rα completely inhibited IL-7 signaling in both $CD4^+$ and $CD8^+$ human T cells (Fig. 3*A*). Consistent with decreased early signaling, as evidenced by diminished STAT-5 phosphorylation, the 500:1 ratio of sIL7Rα:rhIL-7 also diminished IL-7–induced CD127 down-regulation and CD95 up-regulation on day 1 (Fig. 3*B*). However, at later time points, cultures containing sIL7Rα predominantly showed augmented rhIL-7–induced effects, as evidenced by more profound and persistent CD127 down-regulation and CXCR4 up-regulation. Furthermore, IL-7 levels were higher when sIL7Rα was present (Fig. 3*C*), similar to the results observed in the 2E8 model system. These results confirm that sIL7Rα diminishes IL-7 consumption by human T cells, resulting in more potent and prolonged biologic effects.

Interestingly, we observed two exceptions to the pattern of sIL7Rα-mediated potentiation of IL-7 bioactivity. Both CD95 up-regulation and suppressor of cytokine signaling 1 (SOCS1) up-regulation were consistently diminished in the presence of sIL7Rα compared with IL-7 alone, even at late time points

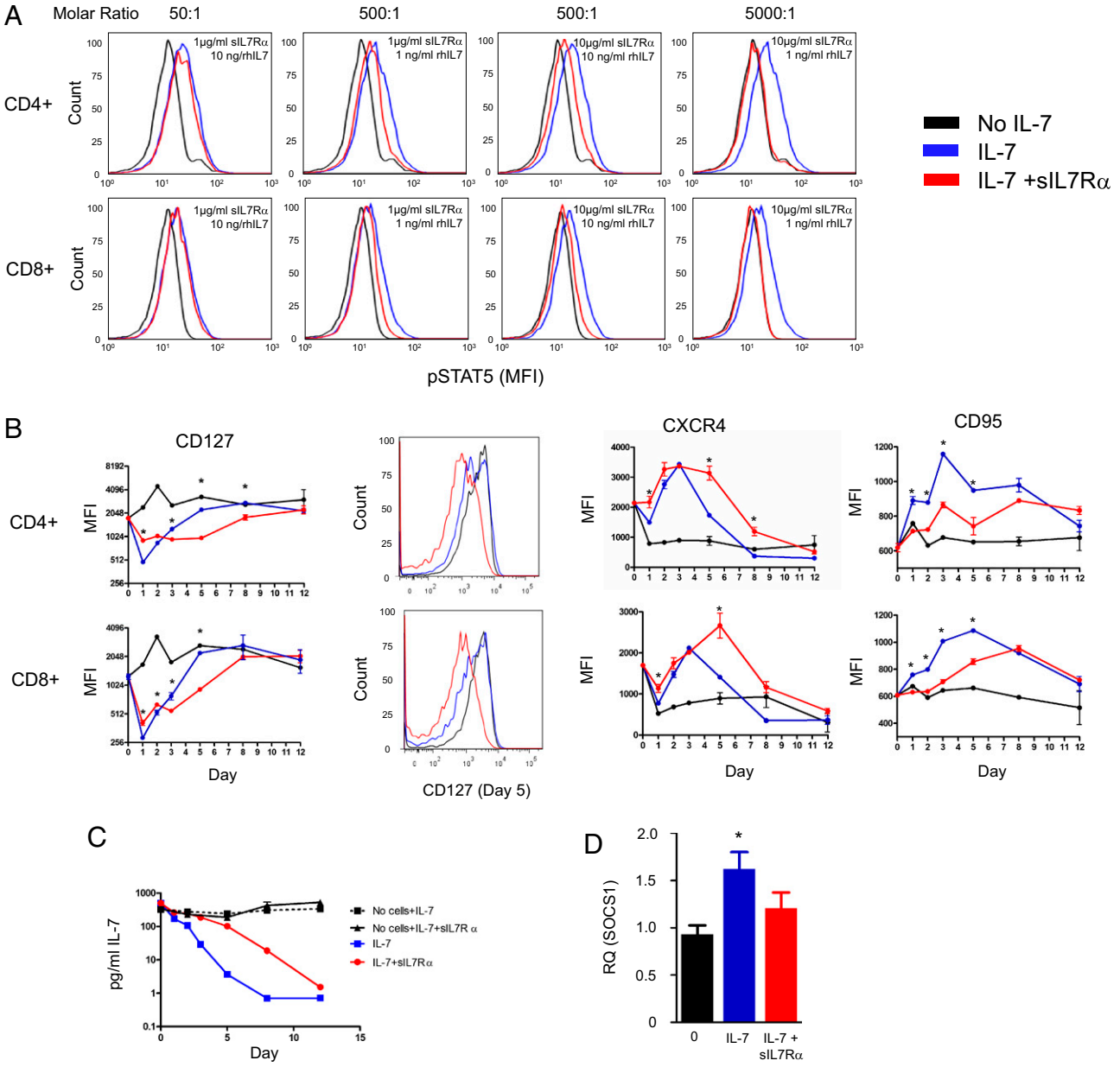

Fig. 3. sIL7Rα-mediated modulation of IL-7 signaling on human T cells leads to diminished IL-7 consumption and diminished SOCS1 and CD95 Induction. Human PBMCs were coincubated with rhIL-7 with or without sIL7Rα and then analyzed at the times shown. Molar ratios were as noted in *A*, whereas 500:1 sIL7Rα:rhIL7 molar ratio was used in *B–D*. (*A*) IL-7–induced STAT-5 phosphorylation was measured in gated $CD4^+$ and $CD8^+$ T cells after 15 min. Cells were serum-starved before IL-7 was added. No effect was seen at 50:1 molar ratio, incomplete inhibition was seen at 500:1 ratio (similar effects at 1 and 10 ng/mL rhIL-7), and complete inhibition was seen at 5,000:1 ratio. Controls using human serum albumin and rat IgG2a at similar concentrations showed no significant impact on STAT-5 signaling. (*B*) Modulation of IL-7–induced changes in CD127, CXCR4, and CD95 expression by sIL7Rα. Representative flow-cytometric histograms of CD127 expression at day 5 on $CD4^+$ and $CD8^+$ T cells are shown on the right. (*C*) IL-7 consumption by human PBMCs is diminished in the presence of sIL7Rα, as measured by ELISA. (*D*) SOCS1 levels are reduced in the presence of sIL7Rα after 24 h of incubation with IL-7. Relative quantity (RQ) of SOCS1/GAPDH mRNA expression compared with untreated cells was determined. Error bars represent 95% CI of triplicate experiments. A total of three independent experiments were performed using PBMCs from different donors with comparable results. Statistical significance shown (*$P < 0.05$) reflects comparisons between rhIL-7 alone and rhIL-7 plus sIL7Rα using a two-tailed *t* test.

(Fig. 3 *B* and *D*). Thus, sIL7Rα also modulates the character of IL-7 signaling by diminishing CD95 and SOCS1, both negative regulators of immune responses, mimicking reduced IL-7 concentration at early time points (Fig. S2). Reduced CD95 expression in the presence of sIL7Rα showed functional significance, as evidenced by reduced anti-Fas–mediated killing compared with IL-7 alone (Fig. S3). Screening for other cytokines in culture supernatants did not reveal any statistically significant differences in IL-1b, IL-2, IL-6, IL-8, IL-10, IL-12p70, GM-CSF, IFNγ, or TNFα production between the culture conditions, suggesting these effects are directly linked to alterations in the IL-7 signal itself. Together, the ability for sIL7Rα to diminish IL-7 consumption and diminish the induction of negative regulators of immune responses led to the prediction that sIL7Rα would potentiate biologic effects of IL-7 in vivo.

sIL7Rα Potentiates IL-7 Bioactivity in Vivo. We next explored the effect of sIL7Rα on IL-7–induced homeostatic expansion in vivo.

IL7$^{-/-}$ mice were chosen for these studies because they provide a lymphopenic milieu within which effects on homeostatic expansion can be readily measured, and they eliminated the possibility of confounded results attributable to signaling by murine IL7. In concordance with our in vitro findings, higher levels of IL-7 were measured 24 h following administration of rhIL-7 with sIL7Rα compared with that measured following administration of rhIL-7 alone ($P < 0.05$ at 24 h; Fig. 4*A*), and coadministration of sIL7Rα with rhIL-7 enhanced rhIL-7–driven homeostatic peripheral expansion of congenic, adoptively transferred lymph node cells, with the most potent effects observed for IL-7–induced CD4$^+$ T-cell expansion (Fig. 4*B*). Thus, similar to the results obtained in vitro, sIL7Rα diminishes clearance of IL-7, resulting in more prolonged exposure and more potent biologic effects.

We next compared the effects of sIL7Rα on IL-7–induced potentiation of experimental autoimmune encephalitis because previous work had demonstrated that coadministration of rhIL7 exacerbates the severity of this disease (12). Myelin oligodendrocyte glycoprotein (MOG)-injected C57BL/6 mice receiving rhIL-7 (5 μg) plus sIL7Rα (100μg) showed significantly worsened experimental autoimmune encephalomyelitis (EAE) symptoms than animals receiving rhIL-7 alone (Fig. 4*C*), as evidenced by an increased mean EAE score for the group as a whole (Fig. 4*C*, *Left*), diminished time to progression to an EAE score of 3 (Fig. 4*C*, *Center*; log-rank $P = 0.03$), and overall disability of individual mice (Fig. 4*C*, *Right*). Thus, sIL7Rα potentiates IL-7–induced exacerbation of autoimmune disease. Interestingly, this effect was observed in nonlymphopenic mice with normal levels of murine IL-7, thus demonstrating that the in vitro-potentiating effects of sIL7Rα on IL7 bioactivity occurred even in the presence of normal levels of murine IL-7, and, thus, the observation is generalizable across several in vitro and in vivo model systems.

IL7R Genotype Modulates sIL7Rα and IL-7 Levels. To validate previous reports of associations between *IL7R* genotype and IL7Rα mRNA splicing (23), we measured Δ6IL7Rα:full-length isoform ratios in resting peripheral blood mononuclear cells (PBMCs) from individuals with *IL7R**CC (autoimmune-predisposing) vs. *IL7R**TT (autoimmune protective) genotypes. The Δ6IL7Rα:full-length ratio was significantly higher in *IL7R**CC vs. *IL7R**TT individuals (mean ± SEM, 0.028 ± 0.001 vs. 0.011 ± 0.001; Fig. 5*A*, *Left*), attributable to an increase in the Δ6IL7Rα isoform (mean ± SEM, 0.78 ± 0.13 vs. 0.33 ± 0.08; Fig. 5*A*, *Right*). We

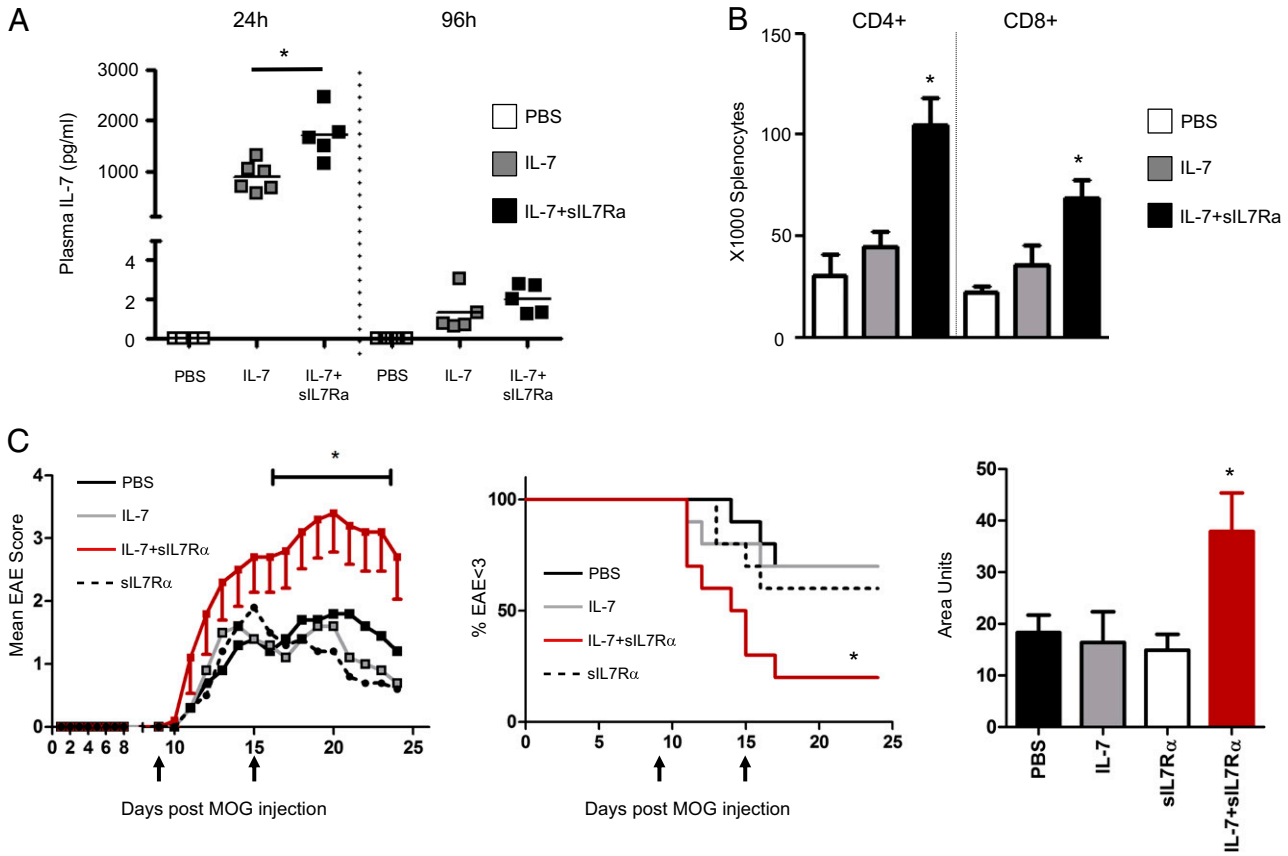

Fig. 4. sIL7Rα diminishes IL-7 clearance in vivo and increases IL-7–mediated homeostatic peripheral expansion. (*A*) On day 0, IL-7$^{-/-}$ mice received one dose of rhIL-7 (5 μg) with or without sIL7Rα (100 μg) coinjected in the same syringe. A 10:1 molar ratio was chosen because of limited availability of recombinant sIL7Rα. Plasma levels were measured at 24 and 96 h. Mice injected with rhIL-7 plus sIL7Rα have higher plasma IL-7 levels after 24 h than those receiving rhIL-7 alone. (*B*) On day 0, mice received IL-7 with or without sIL7Rα, as in *A* above, plus 2×10^6 congenic lymph node cells. On day 8, mice injected with rhIL-7 plus sIL7Rα showed higher numbers of adoptively transferred CD4$^+$ and CD8$^+$ splenocytes compared with mice receiving rhIL-7 alone. Asterisks denote significant differences. These experiments were repeated once for two independent experiments with similar results ($n = 5$ per group). (*C*) C57BL/6 mice ($n = 10$/group) were immunized with MOG and then scored for EAE symptoms. PBS, rhIL-7, sIL7Rα, or rhIL-7 plus sIL7Rα was administered i.p. on days 9 and 15 post-immunization (arrows). Mice injected with rhIL-7 plus sIL7Rα showed increased EAE scores (*Left*), more rapid progression to EAE score 3 (*Center*), and higher overall disability as measured by area under the curve of EAE score over time per individual mouse (*Right*). *$P < 0.05$ as determined by Mann–Whitney test. No significant differences were seen when injecting IL-7 with a control protein (αhIL6Rα) compared with IL-7 alone, using the models shown in *A*, *B*, or *C*. This experiment was carried out three times with similar results.

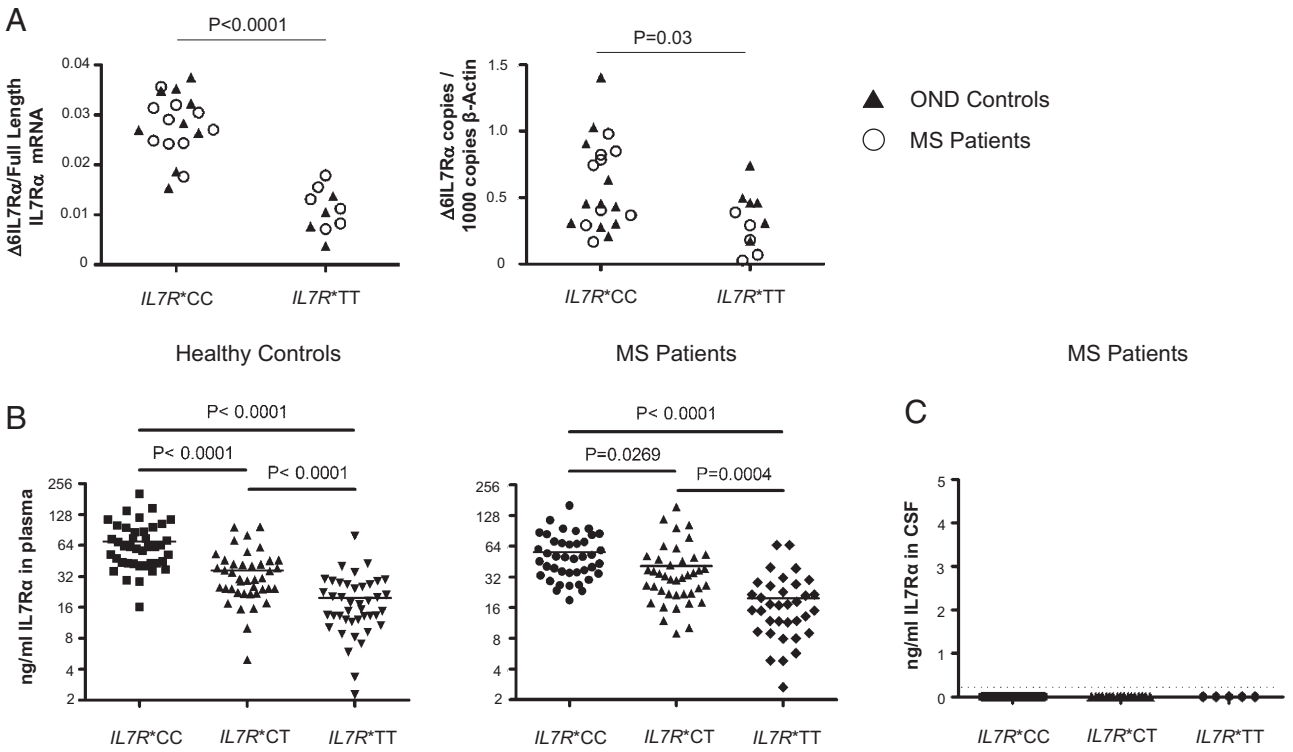

Fig. 5. Individuals with the autoimmunity-associated *IL7R**CC genotype have increased Δ6IL7Rα mRNA and increased levels of circulating sIL7Rα. (*A*) Quantitative, isoform-specific real-time PCR measured Δ6IL7Rα mRNA and full-length IL7Rα mRNA in PBMCs obtained from *IL7R**CC and *IL7R**TT MS patients and controls with ONDs. Each shape represents one patient's sample. *IL7R**CC individuals had increased Δ6IL7Rα/full-length mRNA ratios (*Left*) and increased Δ6IL7Rα mRNA levels (*Right*) compared with *IL7R**TT MS patients and OND controls. (*B*) *IL7R* genotype modulates plasma protein levels of sIL7Rα in healthy controls (n = 41 of each genotype) and MS patients (n = 35–41 of each genotype) as measured using ELISA. The patient and control cohorts analyzed in *B* are distinct from those analyzed in *A*. (*C*) sIL7Rα was not detected in the CSF of MS patients, regardless of genotype. The dotted line indicates detection limit of the assay. *P* values were calculated using an unpaired two-tailed *t* test.

observed no significant difference in the amount of the more plentiful full-length isoform between genotypes. Both MS patients and controls with other neurologic diseases (OND controls) showed a similar pattern, consistent with previous studies in healthy controls (23).

To determine whether genotype influenced sIL7Rα protein levels, we measured circulating IL7Rα levels in *IL7R**CC vs. *IL7R**CT vs. *IL7R**TT individuals (21). Circulating IL7Rα levels in healthy controls (HCs) and MS patients show a wide range [mean (5–95 percentile): HCs, 39.8 ng/mL (7.9–97.4); MS, 42 ng/mL (8.3–111.8)], with an ∼threefold increase in mean sIL7Rα levels in *IL7R**CC vs. *IL7R**TT in HCs [mean (5–95 percentile): *IL7R*CC*, 70.3ng/mL (28.6–146.6); vs. *IL7R*TT*, 19.7 ng/mL (3.7–42.2)] (Fig. 5*B*). We observed a similar ∼threefold increase in mean sIL7Rα in *IL7R**CC vs. *IL7R**TT MS patients (55.8 vs. 19.8 ng/mL), similar to the magnitude of the mRNA increase for the Δ6IL7Rα isoform and the Δ6IL7Rα/IL7Rα full-length ratio (Fig. 5*A*). Heterozygotes (*IL7R**CT) showed intermediate levels of circulating sIL7Rα, implicating an allele-dose effect. sIL7Rα was not measurable in the cerebrospinal fluid (CSF), implying that it does not cross the blood–brain barrier (Fig. 5*C*). This confirms the observations of Hoe et al. (23), who demonstrated previously that *IL7R**CC vs. *IL7R**TT individuals experience increased IL7R mRNA splicing, which leads to increased circulating sIL7Rα. Interestingly, both quantitative PCR and the measured protein levels demonstrate that the autoimmunity predisposing *IL7R*CC* genotype induced an approximately threefold increase in Δ6IL7Rα mRNA levels and in circulating sIL7Rα protein levels.

Given that we clearly observed effects of sIL7Rα on IL-7 consumption in vitro, that previous work has concluded that receptor mediated consumption is a primary mechanism by which IL-7 levels are regulated (36), and that under normal circumstances, IL-7 is considered to be a limited resource (3), we postulated that genotype-induced modulation of sIL7Rα levels could significantly impact IL-7 availability in humans in vivo. To test this, we compared IL-7 levels in plasma and CSF obtained from a cohort of patients with MS (n = 42) classified according to genotype. As shown in Fig. 6*A* (*Left*), we observed significant increases in plasma IL-7 levels among *IL7R**CC MS patients compared with *IL7R**TT patients, consistent with a model wherein increased sIL7Rα leads to diminished consumption and a secondary increase in IL-7 availability. Importantly, we saw no significant effect on CSF IL-7 levels (Fig. 6*A*, *Right*), which is consistent with this model because sIL7Rα is not present in the CNS (Fig. 6*C*). To validate these findings, we screened the larger cohort of MS patients (n = 123) and healthy controls (n = 119) enriched for the *IL7R**TT genotype previously used to determine sIL7Rα levels (Fig. 5*B*). This cohort confirmed a significant effect of *IL7R* genotype on circulating IL-7 levels in patients with MS, such that *IL7R**CC MS patients have, on average, double the mean IL-7 levels (∼8 pg/mL) compared with MS patients with *IL7R**CT or *IL7R**TT genotypes or healthy controls (∼4 pg/mL; Fig. 6*B*). Interestingly, we observed no effect of *IL7R* genotype on IL-7 levels in healthy controls. Serum from both MS cohorts was obtained at the time of disease onset but before initiation of therapy, and, therefore, these findings cannot be attributed to immunosuppressive therapies. What remains to be determined is whether the onset of the autoim-

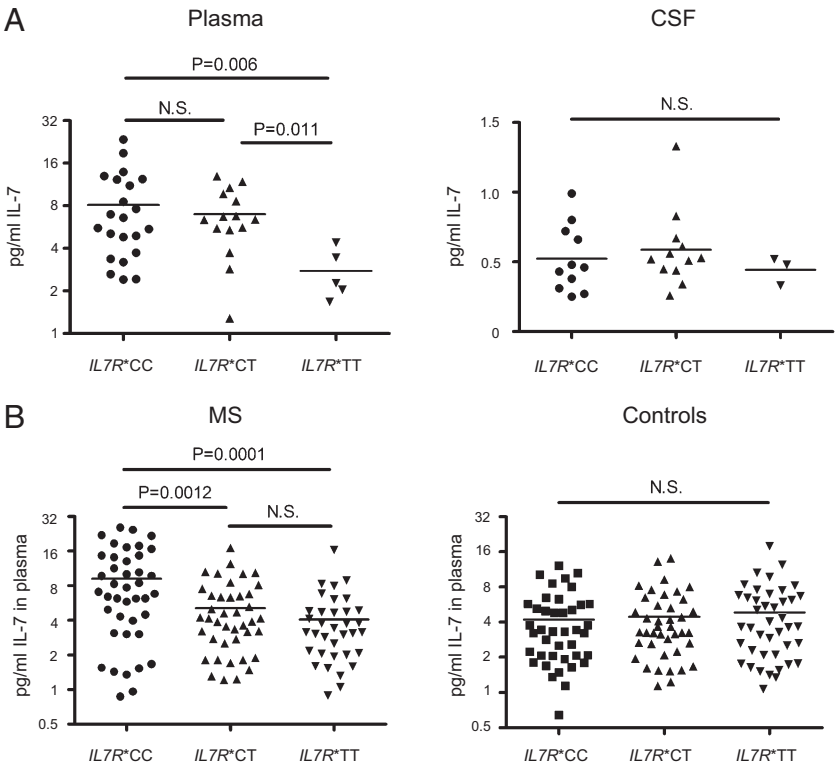

Fig. 6. *IL7R**CC MS patients have increased plasma IL-7 levels. (*A*) IL-7 levels were measured in plasma and CSF from patients with MS according to genotype. *IL7R**CC patients had significantly higher mean plasma IL-7 levels than *IL7R**TT patients, whereas no difference was observed between IL7R*CC and IL7R*CT heterozygotes. No correlation between CSF IL-7 levels and *IL7R* genotype was observed. The dotted line denotes limit of detection. (*B*) Plasma IL-7 levels were measured in plasma from a second independent cohort of patients with MS, as well as a separate cohort of healthy controls. *IL7R**CC MS patients have significantly higher mean IL-7 levels than *IL7R**TT MS patients, whereas no difference was observed according to genotype in healthy controls. Each shape represents a plasma or CSF sample analyzed from one patient or healthy control.

mune disease triggers increased IL-7 levels among *IL7R**CC in MS patients or whether elevations of IL-7 levels in *IL7R**CC MS patients predate the onset of the disease and, thus, potentially predispose to the development of autoimmunity.

Discussion

The biology of soluble receptors is a nascent field in immunology, and both inhibitory and potentiating effects have been reported. Soluble IL2Rα has been reported to both diminish IL-2 signaling (37) and stimulate T-cell growth (38). IL-15 must be bound to either soluble or cell-associated IL15Rα to mediate bioactivity. Soluble IL6R augments IL-6 bioactivity via a novel transsignaling pathway (20, 39). Despite the fact that soluble receptors are known to play an essential role in cytokine biology and the fact that sIL7Rα circulates at high molar excess compared with IL-7 in healthy humans, the biologic effects of sIL7Rα have remained unclear. sIL7Rα was initially reported to block IL-7 signaling (22), but these studies were limited to very early time points and used a chimeric protein consisting of the ECD of IL7Rα linked to human Fc, which binds IL-7 at a lower affinity than native sIL7Rα (Fig. 1). In contrast, coadministration of the same molecule, IL7Rα-Fc, with IL-7 enhanced antitumor effects compared with administration of IL-7 alone in an immunotherapy model of lung cancer in mice (40). Similarly, complexing IL-7 to an anti–IL-7 mAb enhances the potency of IL-7 in murine models (41). Thus, previous work has concluded both inhibitory and potentiating effects of IL-7–binding proteins on IL-7 bioactivity, although no studies have been conducted using the native soluble receptor, which predominates in humans.

This work clearly reconciles published data on this subject, providing a model whereby sIL7Rα binds IL-7 with nanomolar affinity (Fig. 1), thereby diminishing the availability of free IL-7 and modestly competing with cell-associated IL7R, which binds IL-7 with picomolar affinity (34, 35). This competition serves to diminish the potency of early signaling, as evidenced by diminished Stat5 phosphorylation (Fig. 3), but ultimately results in less IL-7 consumption, leading to more prolonged exposure and overall enhanced IL-7 bioactivity in settings where IL-7 availability is limited. The potentiation effects were readily observed in vitro using both a murine IL-7–dependent cell line (Fig. 2), as well as using T cells from healthy human donors (Fig. 3), in the presence of IL-7 concentrations that are standardly used, ranging from 250 pg/mL to 10 ng/mL, but that substantially exceed levels of 2–8 pg/mL, which are present in human serum (42). Thus, the magnitude of the effect could be even more potent than that observed in vitro here, given that IL-7 may be more limited in vivo than in the in vitro models used here. Consistent with the evidence for physiologic relevance of the in vitro observations is the fact that sIL7Rα plus IL-7 administration increased the half-life of IL-7 in vivo, increased IL-7–mediated homeostatic peripheral expansion of lymphocytes during lymphopenia, and worsened the severity of experimental autoimmune encephalitis compared with that in mice receiving IL-7 alone (Fig. 4). Thus, the data overall are consistent with a common theme in studies of soluble cytokine receptor biology and with data using alternative binding proteins for IL-7 (40, 41) in that the data here demonstrate that binding of cytokines to a carrier protein potentiates the biologic activity of the cytokine. The work also rules out the possibility that biologic effects of sIL7Rα occur via modulation of TSLP signaling, because we observed no significant binding between these molecules. We did not observe any effect of sIL7Rα alone administered in the EAE model, but in-

terpretation of this negative result is confounded by potential differences in the affinity of human sIL7Rα to murine IL-7, compared with human IL-7. Future efforts focused on delineating the biology of sIL7Rα in mice could serve as a basis for new models for further study the biology of sIL7Ra in vivo.

In addition to diminished consumption of IL-7 in the presence of sIL7Rα, we also observed changes in IL-7–mediated induction of inhibitory downstream mediators in the presence of sIL7Rα. Whereas Fas (CD95) is up-regulated by IL-7 signaling (43), the degree of Fas up-regulation observed was substantially less in the presence of sIL7Rα (Fig. 3*B*), and this was associated with diminished Fas-induced cell death. Similarly, SOCS1 was readily up-regulated by IL-7 signaling in absence of soluble receptor, but SOCS1 up-regulation was significantly diminished in the presence of receptor (Fig. 3*D*). These results suggest that sIL7Rα also modulates the quality of the IL-7 signal and thereby provide additional mechanisms to explain the observed potentiation of IL-7 bioactivity. Future studies could more fully characterize potential changes in the quality of the IL-7 signal induced by the cytokine in the presence or absence of sIL7Rα and could further explore the contribution of this effect to the potentiation of IL-7 bioactivity via sIL7Rα. In a recent publication by Kimura et al. (44), intermittent IL-7 was shown to deliver a prosurvival signal to T cells compared with continuous IL-7 administration. The factors responsible for this effect may be similar in mechanism to our findings, because both models observe diminished CD95 expression associated with IL-7 signaling. Furthermore, both studies illustrate the complex nature of the IL-7 signal with significant differences in IL-7 bioactivity depending upon modulators of the nature of IL-7 signaling.

This work begins to illuminate the complexity of IL-7 receptor: ligand interactions as they occur in vivo by demonstrating that interactions between IL-7 and its canonical high-affinity, cell-associated receptor are substantially modulated by sIL7Rα, a moderate-affinity binding protein present in high molar excess. Here, we clearly demonstrate potentiating effects of sIL7Rα in vitro with starting molar ratios of 500:1, but these are dynamic because they increase as IL-7 consumption occurs during the culture period. We also saw biologic effects in vivo with much lower starting ratios. Thus, although it is difficult to definitively establish what constitutes a normal, bioactive sIL7Rα:IL7 molar ratio, it is clear that sIL7Rα is present in substantial molar excess under normal conditions in vivo and that the ratios used in these studies, which clearly demonstrate IL-7 potentiation, are well within the range of ratios expected to encountered in vivo. Furthermore, the system is even more complex, given that a small but significant fraction of sIL7Rα is bound to sγc (24) and that IL-7 also binds to glycosaminoglycans in the serum and on the extracellular matrix (45). Homodimers of sIL7Rα are unlikely to make up an additional IL-7–binding complex, given the weak affinity between two IL7Rα extracellular domains (46). Thus, IL-7 encounters a wide array of ligands in vivo, from a low-affinity plentiful sink in tissues, which would characterize extracellular matrix, to a moderate-affinity, plentiful binder characterized by sIL7Rα studied here, to a higher affinity but more limited circulating IL7Rα:sγc heterodimer, and finally to the high-affinity cell-associated IL7R. Despite these complexities, the data presented here using a wide array of model systems, from in vitro cell lines to primary human T cells to murine models and even human studies, consistently demonstrate that sIL7Rα mediates important biologic effects, and the consistent theme is potentiation of IL-7 bioactivity.

Sequencing of the human genome has led to a plethora of genome-wide association studies demonstrating genetic associations with complex diseases (47–49). In most cases, the biologic basis for the genetic association remains unknown, attributable, in part, to the fact that polymorphisms typically induce modest alterations in biology, which are challenging to fully characterize (50, 51). This work explains the biologic basis for the genetic evidence that *IL7R**CC individuals experience increased risk for autoimmunity, in general, and multiple sclerosis, in particular. The data presented confirm previous reports demonstrating a relationship between genotype Δ6IL7Rα mRNA expression and circulating IL7Rα levels. Furthermore, the binding kinetics measured between sIL7Rα and human IL-7 and the levels of sIL7Rα and IL-7 present in the circulation lead to the prediction that even the modest, ∼threefold increase in sIL7Rα levels present in *IL7R**CC compared with *IL7R**TT individuals significantly diminishes free IL-7 in vivo and paradoxically potentiates IL-7 bioactivity by securing sufficient IL-7 levels over time. Consistent with a model whereby genotype induced effects on sIL7Rα modulate IL-7 consumption, we demonstrate that MS patients with *IL7R**CC have higher levels of circulating IL-7. Importantly, this finding was confirmed in two separate cohorts, although we did not see a similar genotype effect in healthy controls. The reason for this distinction remains unclear but deserves further study. It is plausible that early immunologic effects of MS pathogenesis lead to enhanced immune activation that uncovers these genotype-induced effects, and this hypothesis could be tested by evaluating IL-7 levels in other cohorts of patients with autoimmunity according to genotype.

In summary, this work demonstrates that circulating levels of sIL7Rα binds to IL-7 with moderate affinity and competes with the cell-associated IL-7R complex to diminish excessive IL-7 signaling. Because IL-7 is a limited resource whose levels are regulated primarily via receptor-mediated clearance, diminished signaling rates in the presence of sIL7Rα lead to diminished consumption, and overall increases IL-7 bioavailability. Furthermore, sIL7Rα also modulates the quality of the IL-7 signal to diminish the induction of negative regulators. This model predicts, therefore, that the *IL7R**C autoimmunity-predisposing genotype mediates its effect via increased levels of sIL7Rα, which augments IL-7 bioactivity and, thus, predisposes individuals to autoimmunity.

Materials and Methods

Real-Time PCR. Plasmid cDNA standards for each IL7Rα isoform β-actin were synthesized (Mr. Gene). TaqMan gene expression assays specific for the full-length (Hs00904814_m1) and Δ6 (Hs00902337_m1) isoforms were purchased from Applied Biosystems. mRNA was extracted from PBMCs using the RNeasy kit (Qiagen) and transformed into cDNA using the Super script III First Strand Synthesis System (Invitrogen). Genotyping of rs6897932 was carried out using allelic discrimination (Assay ID: C_2025977_10; Applied Biosystems) on an ABI TaqMan 7000 Real-Time PCR machine. SOCS1-relative expression levels were determined by semiquantitative real-time PCR using GAPDH as a housekeeping gene (Assay ID: SOCS1, Hs00705164_s1; GAPDH, Hs02758991_g1; Applied Biosystems).

Human Samples. All patient and control samples were acquired after written consent was obtained and the use of samples was approved by the regional ethical review board at Karolinska Institutet. Human plasma samples were obtained from two different Swedish cohorts: the first is from the Epidemiological Investigation of Multiple Sclerosis (52) (Figs. 5*B* and 6*B*), in which MS patients' plasma was collected at diagnosis (according to McDonald criteria), in patients between 16–70 y of age from different Swedish clinics. Healthy controls were selected from an age- and geographically matched control cohort based on *IL7R* genotype. The second was from the Stockholm Prospective Assessment Study of MS (Figs. 5 *A* and *C* and 6*A*), in which plasma and CSF and PBMC samples were collected from MS patients at diagnosis, but before any MS-directed therapy at the Karolinska University Hospital, Stockholm, Sweden. Controls with ONDs were visitors to the same hospital but confirmed by clinic neurologists as not having MS. PBMCs from healthy controls were obtained from healthy blood donors via the National Institutes of Health (NIH) Department of Transfusion Medicine, who underwent informed consent according to NIH Clinical Center Institutional Review Board approved protocols. Plasma, cDNA, and CSF samples were stored at −80 °C and shipped on dry ice before analyses.

ELISAs. Human IL-7 levels in human plasma, mouse plasma, and culture supernatants were measured by high-sensitivity IL-7 ELISA kit according to

the manufacturer's instructions (Quantikine; R&D Systems). Plasma IL7Rα levels were measured by a custom-made validated ELISA as described previously (21).

Protein Production-Affinity Measurements. Human IL-7 was expressed from *Escherichia coli* and purified as described previously (53). The human IL7R ECD was expressed from *Drosophila* Schneider 2 (S2) insect cells and purified as described previously (53). The sIL7Rα gene (residues 23–254; UniProt accession no. P31785) was cloned into the BglII and EcoRI restriction sites of the transfer vector pMT-BipA (Invitrogen) and subsequently confirmed by DNA sequencing. The sIL7Rα construct contains an extra Arg-Ser and an eight-residue His tag at the N-terminal end. A stable S2 insect cell line secreting sIL7Rα was generated, and the protein was expressed and purified using similar methods described previously for the IL7Rα-ECD (53). The human TSLP cDNA was purchased from Origene, cloned into the NcoI and BamHI restriction sites of the pET-15b expression vector, confirmed by DNA sequencing, and expressed in *E. coli*. The TSLP construct contains an extra M-G at the N-terminal end. TSLP was expressed and purified using similar procedures described for IL-7 (53). Human TSLPR fused as an F_c chimera expressed from NS0 cells was purchased from R&D Systems and was used without further purification. Molar absorption coefficients at 280 nm of 6.9, 16.6, 31.9, and 38.8 mM/cm were used to determine protein concentrations of IL-7, TSLP, IL7Rα-EC, and sIL7Rα, respectively (54).

Protein Production-Functional Studies. Δ6IL7Rα cDNA was synthesized to order based on the GenBank accession no. AK301220 sequence by Mr. Gene. The Δ6IL7Rα protein was purified from supernatant obtained from HEK293E cells transiently expressed with a 7.1-kb mammalian expression clone containing the Δ6IL7Rα cDNA sequence flanked by the CMV promoter and His6. Δ6IL7Rα protein was purified from culture supernatant by immobilized metal ion-affinity chromatography.

Surface Plasmon Resonance. Experiments were performed using a Biacore 3000 SPR instrument at 25 °C. IL-7Rα-ECD, sIL7Rα, and TSLPR coupling and binding kinetics were measured using a CM5 sensor chip. The receptors were amine-coupled to the sensor chip using previously described methods (55). Experiments were performed in 10 mM Hepes (pH 7.4), 150 mM NaCl, 3 mM EDTA, and 0.005% Tween-20 at 25 °C. Binding kinetics of the association between the cytokines and receptors were performed with a flow rate of 50 μL/min. Twofold serial dilutions of differing cytokine concentrations were assayed. Each 250-μL protein or buffer injection was followed by a 40-s dissociation period. Surfaces were regenerated for subsequent runs with a 5-μL injection of 4 M $MgCl_2$.

Sensorgrams were trimmed and double-referenced (56) using BIAevaluation Version 4.1 (BiaCore). Global-fitting analysis of the sensorgrams used the program ClampXP (57). Experiments were performed in triplicate, and errors were propagated using Taylor series expansion (58). All of the binding interactions fit best to a two-step (three-state) reaction model (55) originally described for SPR analysis (56). Apparent equilibrium dissociation constants (K_d) were calculated using the following equation: $K_d = k_{-1}k_{-2}/k_1(k_2 + k_{-2})$.

In Vitro Culture. The 2E8 cells (IL-7–dependent murine pro–B-cell line) and human PBMCs were cultured in media supplemented with a single dose of IL-7 and sIL7Rα at the concentrations indicated. Cell counts were carried out using a Z2 cell counter (Beckman Coulter), and viability was determined by 7AAD gating via flow cytometry. Flow-cytometric analysis was carried out on a FACS LSRFortessa (Becton-Dickinson) using fluorochrome-labeled staining antibodies (listed below). For Stat5 phosphorylation assays, human PBMCs were serum-starved overnight and given a single dose of IL-7 with or without sIL7Ra, and 15 min later, cells were fixed (Fix Buffer I; BD Biosciences) and permeabilized (Perm buffer III), and then anti-Stat5 phosphoantibodies were added according to the manufacturer's instructions.

Mouse Experiments. All studies were conducted according to National Cancer Institute Animal Care and Use Committee-approved protocols. $IL7^{-/-}$, $CD45.2^+$ female mice were injected with 2×10^6 $CD45.1^+$ lymph node cells plus 5 μg of rhIL-7 (CYT107; Cytheris SA) with or without 100 μg of sIL7Rα. Mice were humanely euthanized on day 8, and then total splenocyte counts were determined by homogenizing mouse spleen using a GentleMACS Dissociator (Miltenyi Biotech), lysing red cells (ACK lysing buffer, Lonza), and counting using a Coulter counter. In parallel, $IL7^{-/-}$ male mice were injected with the same amounts of rhIL-7 with or without sIL7Rα without lymphocytes. Plasma IL-7 levels were determined at days 1 and 4 following retro-orbital blood collection.

For the EAE studies, female C57BL/6 mice were immunized by two s.c. injections of 200 μg of MOG_{35-55} (American Peptide Company) emulsified in Complete Freund's Adjuvant containing 5 mg/mL H37Ra (Chondrex) in both flanks near the tail base; 400 ng of pertussis toxin (Sigma-Aldrich) was given i.p. on days 0 and 2 post MOG injection. On days 9 and 15, PBS, 5 μg of IL-7, 100 μg of sIL7Rα, 5 μg of IL-7 plus 100 μg of sIL7Rα, or 5 μg of IL-7 plus 100 μg of hαIL6Rα (control protein) was injected i.p. (n = 10 per group). Mice were scored daily by blinded observers starting on day 8 using the following system: 0, normal; 1, flaccid tail, no paraparesis; 2, hind-limb weakness evidenced by inability to right itself when placed on the back, or inability to grasp with its hind limbs; 3, partial hind limb paralysis evidenced by inability to move one hind limb (e.g., to withdraw one limb when pinched but able to bear weight on one limb); 4, complete hind-limb paralysis evidenced by inability to move or withdraw limb; and 5, quadriplegia evidenced by inability to move front and hind limbs (humane end point).

Statistical Analyses. Graphs represent mean values ± SEM. P values were calculated as indicated in each respective figure using Student's t test or the Mann–Whitney U test. $P < 0.05$ was considered statistically significant and is illustrated with an asterisk in the figures.

ACKNOWLEDGMENTS. We thank Drs. Al Singer, Scott Durum, and Hyun Park for careful review of this manuscript and helpful discussions. This work was supported, in part, by the Intramural Research Program of the National Institutes of Health (NIH). S.T.R.W. was supported by NIH Grant AI72142.

1. Tan JT, et al. (2001) IL-7 is critical for homeostatic proliferation and survival of naive T cells. *Proc Natl Acad Sci USA* 98(15):8732–8737.
2. Schluns KS, Kieper WC, Jameson SC, Lefrançois L (2000) Interleukin-7 mediates the homeostasis of naïve and memory CD8 T cells in vivo. *Nat Immunol* 1(5):426–432.
3. Park JH, et al. (2004) Suppression of IL7Ralpha transcription by IL-7 and other prosurvival cytokines: A novel mechanism for maximizing IL-7-dependent T cell survival. *Immunity* 21(2):289–302.
4. Goldrath AW, Bevan MJ (1999) Low-affinity ligands for the TCR drive proliferation of mature CD8+ T cells in lymphopenic hosts. *Immunity* 11(2):183–190.
5. Ernst B, Lee DS, Chang JM, Sprent J, Surh CD (1999) The peptide ligands mediating positive selection in the thymus control T cell survival and homeostatic proliferation in the periphery. *Immunity* 11(2):173–181.
6. Guimond M, et al. (2009) Interleukin 7 signaling in dendritic cells regulates the homeostatic proliferation and niche size of CD4+ T cells. *Nat Immunol* 10(2):149–157.
7. Sportès C, et al. (2010) Phase I study of recombinant human interleukin-7 administration in subjects with refractory malignancy. *Clin Cancer Res* 16(2):727–735.
8. Fry TJ, et al. (2003) IL-7 therapy dramatically alters peripheral T-cell homeostasis in normal and SIV-infected nonhuman primates. *Blood* 101(6):2294–2299.
9. McHugh RS, Shevach EM (2002) Cutting edge: Depletion of CD4+CD25+ regulatory T cells is necessary, but not sufficient, for induction of organ-specific autoimmune disease. *J Immunol* 168(12):5979–5983.
10. Calzascia T, et al. (2008) CD4 T cells, lymphopenia, and IL-7 in a multistep pathway to autoimmunity. *Proc Natl Acad Sci USA* 105(8):2999–3004.
11. Uehira M, Matsuda H, Nakamura A, Nishimoto H (1998) Immunologic abnormalities exhibited in IL-7 transgenic mice with dermatitis. *J Invest Dermatol* 110(5):740–745.
12. Liu X, et al. (2010) Crucial role of interleukin-7 in T helper type 17 survival and expansion in autoimmune disease. *Nat Med* 16(2):191–197.
13. Lee LF, et al. (2011) IL-7 promotes T(H)1 development and serum IL-7 predicts clinical response to interferon-β in multiple sclerosis. *Sci Transl Med* 3(93):93ra68.
14. Tomita T, et al. (2008) Colitogenic CD4+ effector-memory T cells actively recirculate in chronic colitic mice. *Inflamm Bowel Dis* 14(12):1630–1640.
15. Penaranda C, et al. (2012) IL-7 receptor blockade reverses autoimmune diabetes by promoting inhibition of effector/memory T cells. *Proc Natl Acad Sci USA* 109(31):12668–12673.
16. Gonzalez-Quintial R, et al. (2011) Systemic autoimmunity and lymphoproliferation are associated with excess IL-7 and inhibited by IL-7Rα blockade. *PLoS ONE* 6(11):e27528.
17. Heaney ML, Golde DW (1996) Soluble cytokine receptors. *Blood* 87(3):847–857.
18. Giri JG, et al. (1994) Elevated levels of shed type II IL-1 receptor in sepsis. Potential role for type II receptor in regulation of IL-1 responses. *J Immunol* 153(12):5802–5809.
19. Peters M, et al. (1996) The function of the soluble interleukin 6 (IL-6) receptor in vivo: Sensitization of human soluble IL-6 receptor transgenic mice towards IL-6 and prolongation of the plasma half-life of IL-6. *J Exp Med* 183(4):1399–1406.
20. Bergamaschi C, et al. (2012) Circulating IL-15 exists as heterodimeric complex with soluble IL-15Rα in human and mouse serum. *Blood* 120(1):e1–e8.
21. Janot-Sardet C, Assouline B, Cheynier R, Morre M, Beq S (2010) A validated assay to measure soluble IL-7 receptor shows minimal impact of IL-7 treatment. *J Immunol Methods* 353(1-2):115–123.
22. Crawley AM, Faucher S, Angel JB (2010) Soluble IL-7R alpha (sCD127) inhibits IL-7 activity and is increased in HIV infection. *J Immunol* 184(9):4679–4687.

23. Hoe E, et al. (2010) Functionally significant differences in expression of disease-associated IL-7 receptor alpha haplotypes in CD4 T cells and dendritic cells. *J Immunol* 184(5):2512–2517.
24. Rose T, Lambotte O, Pallier C, Delfraissy JF, Colle JH (2009) Identification and biochemical characterization of human plasma soluble IL-7R: Lower concentrations in HIV-1-infected patients. *J Immunol* 182(12):7389–7397.
25. Peschon JJ, et al. (1998) An essential role for ectodomain shedding in mammalian development. *Science* 282(5392):1281–1284.
26. Renauld JC, et al. (1992) Expression cloning of the murine and human interleukin 9 receptor cDNAs. *Proc Natl Acad Sci USA* 89(12):5690–5694.
27. Gregory SG, et al.; Multiple Sclerosis Genetics Group (2007) Interleukin 7 receptor alpha chain (IL7R) shows allelic and functional association with multiple sclerosis. *Nat Genet* 39(9):1083–1091.
28. Lundmark F, et al. (2007) Variation in interleukin 7 receptor alpha chain (IL7R) influences risk of multiple sclerosis. *Nat Genet* 39(9):1108–1113.
29. Hafler DA, et al.; International Multiple Sclerosis Genetics Consortium (2007) Risk alleles for multiple sclerosis identified by a genomewide study. *N Engl J Med* 357(9): 851–862.
30. Sawcer S, et al.; International Multiple Sclerosis Genetics Consortium; Wellcome Trust Case Control Consortium 2 (2011) Genetic risk and a primary role for cell-mediated immune mechanisms in multiple sclerosis. *Nature* 476(7359):214–219.
31. Lundström W, Fewkes NM, Mackall CL (2012) IL-7 in human health and disease. *Semin Immunol* 24(3):218–224.
32. Hoe E, et al. (2010) Interleukin 7 receptor alpha chain haplotypes vary in their influence on multiple sclerosis susceptibility and response to interferon Beta. *J Interferon Cytokine Res* 30(5):291–298.
33. Goodwin RG, et al. (1990) Cloning of the human and murine interleukin-7 receptors: Demonstration of a soluble form and homology to a new receptor superfamily. *Cell* 60(6):941–951.
34. Noguchi M, et al. (1993) Interleukin-2 receptor gamma chain: A functional component of the interleukin-7 receptor. *Science* 262(5141):1877–1880.
35. Park LS, Friend DJ, Schmierer AE, Dower SK, Namen AE (1990) Murine interleukin 7 (IL-7) receptor. Characterization on an IL-7-dependent cell line. *J Exp Med* 171(4): 1073–1089.
36. Hodge JN, et al. (2011) Decreases in IL-7 levels during antiretroviral treatment of HIV infection suggest a primary mechanism of receptor-mediated clearance. *Blood* 118(12):3244–3253.
37. Cabrera R, et al. (2010) Hepatocellular carcinoma immunopathogenesis: Clinical evidence for global T cell defects and an immunomodulatory role for soluble CD25 (sCD25). *Dig Dis Sci* 55(2):484–495.
38. Maier LM, et al. (2009) Soluble IL-2RA levels in multiple sclerosis subjects and the effect of soluble IL-2RA on immune responses. *J Immunol* 182(3):1541–1547.
39. Waetzig GH, Rose-John S (2012) Hitting a complex target: An update on interleukin-6 trans-signalling. *Expert Opin Ther Targets* 16(2):225–236.
40. Andersson A, et al. (2011) Role of CXCR3 ligands in IL-7/IL-7R alpha-Fc-mediated antitumor activity in lung cancer. *Clin Cancer Res* 17(11):3660–3672.
41. Boyman O, Ramsey C, Kim DM, Sprent J, Surh CD (2008) IL-7/anti-IL-7 mAb complexes restore T cell development and induce homeostatic T Cell expansion without lymphopenia. *J Immunol* 180(11):7265–7275.
42. Fry TJ, et al. (2001) A potential role for interleukin-7 in T-cell homeostasis. *Blood* 97(10):2983–2990.
43. Fluur C, et al. (2007) Potential role for IL-7 in Fas-mediated T cell apoptosis during HIV infection. *J Immunol* 178(8):5340–5350.
44. Kimura MY, et al. (2013) IL-7 signaling must be intermittent, not continuous, during $CD8^+$ T cell homeostasis to promote cell survival instead of cell death. *Nat Immunol* 14(2):143–151.
45. Ariel A, et al. (1997) Induction of T cell adhesion to extracellular matrix or endothelial cell ligands by soluble or matrix-bound interleukin-7. *Eur J Immunol* 27(10): 2562–2570.
46. McElroy CA, et al. (2012) Structural reorganization of the interleukin-7 signaling complex. *Proc Natl Acad Sci USA* 109(7):2503–2508.
47. Manolio TA, et al. (2009) Finding the missing heritability of complex diseases. *Nature* 461(7265):747–753.
48. Manolio TA (2010) Genomewide association studies and assessment of the risk of disease. *N Engl J Med* 363(2):166–176.
49. Visscher PM, Montgomery GW (2009) Genome-wide association studies and human disease: From trickle to flood. *JAMA* 302(18):2028–2029.
50. Ginsburg D (2011) Genetics and genomics to the clinic: A long road ahead. *Cell* 147(1): 17–19.
51. Hindorff LA, et al. (2009) Potential etiologic and functional implications of genome-wide association loci for human diseases and traits. *Proc Natl Acad Sci USA* 106(23): 9362–9367.
52. Hedström AK, Bäärnhielm M, Olsson T, Alfredsson L (2009) Tobacco smoking, but not Swedish snuff use, increases the risk of multiple sclerosis. *Neurology* 73(9):696–701.
53. Wickham J, Jr., Walsh ST (2007) Crystallization and preliminary X-ray diffraction of human interleukin-7 bound to unglycosylated and glycosylated forms of its alpha-receptor. *Acta Crystallogr Sect F Struct Biol Cryst Commun* 63(Pt 10):865–869.
54. Pace CN, Vajdos F, Fee L, Grimsley G, Gray T (1995) How to measure and predict the molar absorption coefficient of a protein. *Protein Sci* 4(11):2411–2423.
55. McElroy CA, Dohm JA, Walsh ST (2009) Structural and biophysical studies of the human IL-7/IL-7Ralpha complex. *Structure* 17(1):54–65.
56. Morton TA, Myszka DG, Chaiken IM (1995) Interpreting complex binding kinetics from optical biosensors: A comparison of analysis by linearization, the integrated rate equation, and numerical integration. *Anal Biochem* 227(1):176–185.
57. Morton TA, Myszka DG (1998) Kinetic analysis of macromolecular interactions using surface plasmon resonance biosensors. *Methods Enzymol* 295:268–294.
58. Bevington PR, Robinson DK (2003) *Data Reduction and Error Analysis for the Physical Sciences* (McGraw Hill, Burr Ridge, IL).